Resonant-enhanced dipolar interaction between THz-photons and confined acoustic phonons in nanostructures

Tzu-Ming Liu[a], Ja-Yu Lu[a], Chung-Chiu Kuo[a], Meng-Ju Yang[b], Chih-Wei Lai[b], Pi-Tai Chou[b], Ming-Hao Chang[c], Hsiang-Lin Liu[c], Yu-Tai Li[d], Ci-Ling Pan[d], Shih-Hung Lin[e], Chieh-Hsiung Kuan[e], and Chi-Kuang Sun* [a,f,]

[a] Graduate Institute of Photonics and Optoelectronics, National Taiwan University, Taipei 10617, Taiwan R.O.C. [b]Department of Chemistry, National Taiwan University, Taipei 10617, Taiwan R.O.C. [c]Department of Physics, National Taiwan Normal University, Taipei 11650, Taiwan R.O.C. [d]Department of Photonics, National Chiao Tung University, Hsinchu 300, Taiwan R.O.C [e]Department of Electrical Engineering, National Taiwan University, Taipei 10617, Taiwan R.O.C. [f]National Taiwan University, and Research Center for Applied Sciences, Academia Sinica, Taipei 10617, Taiwan R.O.C.

ABSTRACT

By using a frequency-controlled narrow band THz source, a Fourier Transform Infrared (FTIR) spectroscopy system, and a frequency-controlled terahertz (THz) emitter, for the first time, we studied the THz photon absorption related to the THz confined acoustic vibrations in semiconductor nanocrystals. Through a specific charge separation in the CdSe/CdTe type-II nanocrystals and a piezoelectric coupling in the wurtzite CdSe nanocrystals, the THz photons can be resonantly coupled with (l=1) dipolar modes and the (l=0) breathing modes, respectively. Our results provide new mechanisms for low dimensional systems to convert a THz photon into a phonon of the same frequency.

Keywords: Terahertz, confined acoustic phonons, type-II nanocrystals, piezoelectric nanocrystals

1. INTRODUCTION

With spatial confinement, low dimensional systems such as quantum dots and nano-wires exhibit not only electronic but also acoustic energy quantization. In 1882, H. Lamb had already studied the acoustic modes confined in a homogeneous free sphere.[1] Two types of modes, torsional (TOR) and spheroidal (SPH), are derived from the stress-free boundary condition on the spherical surface. According to the selection rules,[2] THz absorption spectroscopy can reveal SPH modes with odd quantum number of angular momentum l, which is not experimentally examined until a recent report by Murray *et al.*.[3] They measured an excess THz absorption of TiO_2 nanopowders and proposed it results from dipolar interaction with (SPH, l=1) confined acoustic modes. Using a simple electro-mechanical model, they suspected the permanent charges required for activating THz absorption came from the adsorbed water molecules.[3] For further investigation and verification, here we synthesized CdSe/CdTe (core-shell) type-II nanocrystals (NCs) as a template with specific core-shell charge separation.[4] After measuring the THz absorption spectrum, we found the frequency of resonant absorption agrees with that of (SPH, l=1) modes predicted by elastic continuum theory. Besides, the cross section of excess THz absorption σ_{ex} shows D^4 dependence on the particle diameter D, indicating the charges was contributed from the surface-defect related donors. Our results not only support Murray's electro-mechanical model[3] but also directly prove the existence of resonant-enhanced dipolar interaction between THz-photons and (SPH, l=1) confined acoustic phonons in NCs.

Furthermore, if the nanocrystals have intrinsic piezoelectricity, without the help of foreign charges,[3] the confined acoustic vibrations should fluctuate the dipole-moment of nanocrystals and also couple with the incident THz photons. Therefore, in this work, we also report the first observation of piezoelectricity induced THz photon absorption related to the confined acoustic phonons in nanoparticles. By using a Fourier Transform Infrared (FTIR) spectroscopy system we measured the THz absorption spectra of wurtzite (piezoelectric) CdSe nanocrystals. The THz photon inactive (l=0) breathing modes were found to become THz photon active in wurtzite CdSe nanocrystals due to the piezoelectric

Ultrafast Phenomena in Semiconductors and Nanostructure Materials XII
edited by Jin-Joo Song, Kong-Thon Tsen, Markus Betz, Abdulhakem Y. Elezzabi
Proc. of SPIE Vol. 6892, 68921C, (2008) · 0277-786X/08/$18 · doi: 10.1117/12.760547

coupling. The frequency of the measured resonant absorption was inversely proportional to the size of the CdSe nanocrystals. This piezoelectric coupled electric vibration provides a new mechanism for low dimensional systems to convert a THz photon into a phonon of the same frequency.

2. THZ PHOTON ABSORPTION BY TYPE-II NANOCRYSTALS

The distribution of the displacement vector of the [SPH, l=1,n=0] and [SPH, l=1,n=1] dipolar modes in a nanosphere have been simulated in Ref. 3, where n is the mode index. They both have relative displacement between the center (core) and the outer (shell) regions. Therefore, a core-shell charge separation is required to match the motional pattern, to induce the change of dipole moment, and to activate the resonant absorption of [SPH, l=1] dipolar modes. However, it is hard for inorganic clusters to create specific and long term charge separation. Besides, the amount of charge should be large enough to induce detectable excess absorption over the background dielectric absorption.[5] That could be the main reason why the report is rare for THz absorption related to [SPH, l=1] modes. Following these properties and requirements, we prepared CdSe/CdTe (core/shell) type-II nanocrystals by chemical synthesis.[6] Due to a large surface to volume ratio, the surface lone-pairs on the Tellurium dangling bonds[7] could be thermally or optically excited to the conduction band of CdTe and then fall into the CdSe core with lower electric potential. This process can result in negatively charged core and a positively charged ion shell on the CdTe surface. This specific core-shell charge separation should enable the studies of the dipolar interaction between THz photons and confined acoustic modes in NCs.

The synthesis of CdSe/CdTe NCs follows the step in a previous work.[6] The NCs were precipitated by the addition of methanol to the cooled, room temperature reaction mixture. After centrifugation and drying under nitrogen flow, the powders were obtained. With this procedure, we synthesized 3.6×10^{15}, 1.4×10^{16}, and 1.6×10^{16} particles of 8nm (4.3nm core) (Fig. 1(a)), 10.4nm (4.3nm core) (Fig. 1(b)), and 13nm (5.3nm core) (Fig. 1(c)) CdSe/CdTe type-II NCs. From transmission electron microscope (TEM) images (Fig. 1(a)-(c)), it was determined that the standard deviation of their sizes was ~±20%. Figure 1(d) shows the absorption (gray curve) and emission (black curve) spectra of the 8nm samples. The absorption spectra didn't show steep absorption edges while smoothly extended to red and near infrared. The emission spectrum peaks around 1048nm. For 10nm and 13nm samples, they all show the same absorption features and similar emission peaks around 1100nm. The infrared emission of all samples indicates a recombination between CdSe electrons and CdTe holes, which validates the presence of type-II band alignment in our samples. These NC powders were separately sealed between two 30-μm thick poly-ethylene (PE) films for the convenience of holding in the THz absorption spectroscopy system.

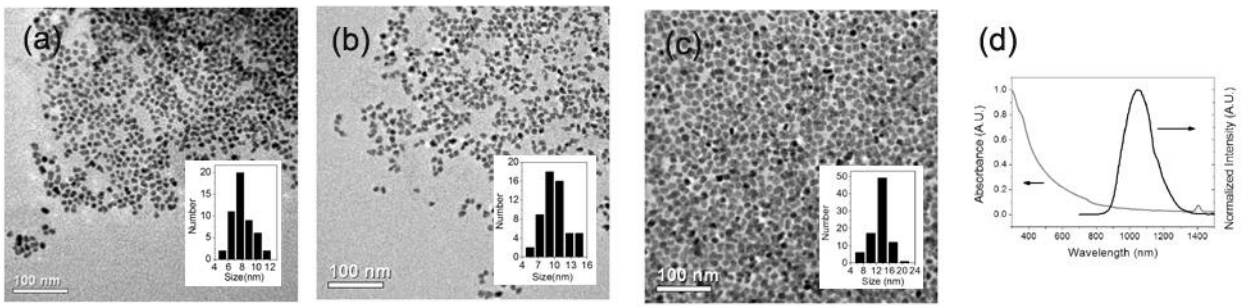

Fig 1. The transmission electron microscope images of (a) 8nm, (b) 10.4nm, and (c) 13nm CdSe/CdTe nanocrystals. (d) The absorption (gray curve) and emission (black curve) spectra of 8nm CdSe/CdTe nanocrystals.

The experimental setup for the THz absorption spectroscopy is similar to a previous work.[8] We employed an edge-coupled membrane photonic transmitter to generate quasi-continuous-wave THz pulses with a tunable central frequency. The radiated THz wave was collected by two off-axis parabolic reflectors and then focused on a bolometer. The sample of the nanocrystals was put in front of the bolometer for the measurement of the THz absorption spectra. Figure 2(a) (solid curve) shows the emission spectrum of the frequency tunable THz emitter after the PE film without CdSe/CdTe

NCs. The spectral power reached a maximum at 100GHz and extended to 400GHz with a substantial signal to noise ratio. With the PE film containing 13nm CdSe/CdTe NCs, the measured THz power spectrum shows obvious attenuation (dotted curve in Fig. 2(a)). Dividing these two data sets, we calculated the extinction cross section for excess THz absorption of each NC by $\sigma_{ex} = \ln(T)A/N$, where T is the transmission, A is the excitation area, and N is the number of nanocrystals in the excitation area. The spectrum of the extinction cross section σ_{ex} shows a 165±40 GHz peak (Fig. 2(b)). The absorption feature was smeared, not only due to the nonuniform particle size, but possibly also due to other physical mechanisms such as interparticle interactions and the large resolution bandwidth of our THz source (~50GHz). Then we performed similar measurement on 10.4nm and 8nm NCs. For 10.4nm NCs, we measured two absorption peaks of 200±40GHz and 360±70GHz (See Fig. 2(c)). While for 8nm NCs, we measured the only 210GH±31GHz peak (See Fig. 2(d)). To ensure if the absorption bandwidth was limited by the coherent controlled THz source, we also double checked the dipolar mode induced THz absorption on 10.1nm CdSe/CdTe NCs with a THz time domain spectroscopy (TDS) system.[9] The spectral resolution is 10GHz and the spectrum of extinction cross section shows absorption peaks at 175±34GHz and 322±32GHz (See Fig. 2(e)). For the fundamental mode, the ratio of peak wavelength over linewidth is 2.6, which is close to that caused by ±20% size variation. We thus attribute the broadening of the absorption band to the size non-uniformity of nanocrystals.

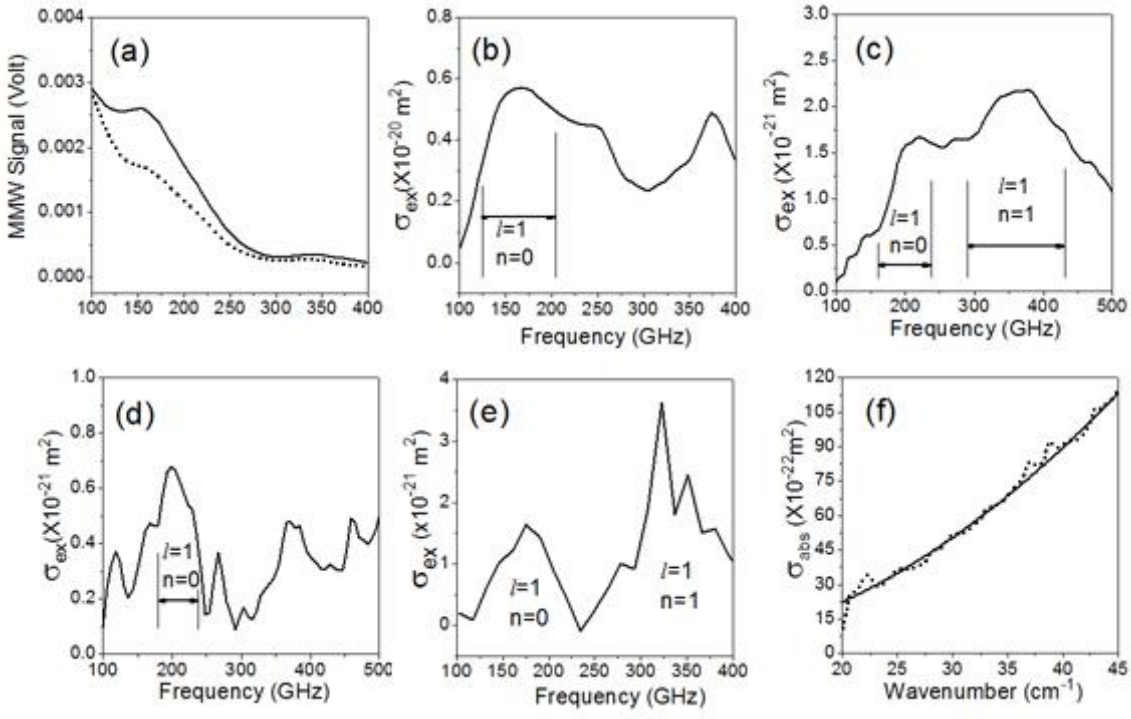

Fig 2. (a) Power spectra after PE film with (dotted line) and without (solid line) 13nm CdSe/CdTe nanocrystals. The spectra of the extinction cross section σ_{ex} of (b)13nm, (c)10.4nm, (d)8nm, and (e)10.1nm CdSe/CdTe nanocrystals. (f) The spectrum of extinction cross section related to the dielectric absorption of 10.4nm CdSe/CdTe nanocrystals (dotted curve).

To check the agreement of resonant frequency with theory, we calculate the eigen frequency ν of (SPH, l=1) modes by the eigen value equation with l=1:[1]

$$4\frac{j_2(\xi)}{j_1(\xi)}\xi - \eta^2 + 2\frac{j_2(\eta)}{j_1(\eta)}\eta = 0, \qquad (1)$$

where $\xi = \pi\nu D/V_L$, $\eta = \pi\nu D/V_T$, and $j_l(\eta)$ is the spherical Bessel function of the first kind;. V_L and V_T are the sound velocities of longitudinal and transverse waves, respectively. Because the acoustic properties of CdSe and CdTe are very similar,[10] we treat the NCs acoustically as CdSe spheres. Using the acoustic parameters of CdSe (V_L= 3570 m/s,

V_T=1720 m/s)[10] the frequency of (SPH, l=1, n=0) modes calculated for 13nm CdSe/CdTe NCs is 152GHz. Considering the resolution of our source and the uncertainties in the size distribution, the frequency of our extinction peak agrees with theoretical prediction. At the frequency of peak absorption, the transmitted THz power decayed to 0.65 of the original, corresponding to ~5.7×10^{-21} m^2 of σ_{ex}. To make sure if there are contribution from background dielectric absorption, we also measured the absorption spectrum of 10.4nm nanocrystals by Fourier Transform Infrared (FTIR) Spectroscopy (See Fig. 2(f), dotted curve). It shows a typical quadratic dependence of dielectric absorption on the frequency of electromagnetic waves.[5] By quadratic curve fitting (See Fig. 2(f), solid curve) and extrapolation from the FTIR data, the corresponding dielectric absorption cross section σ_{abs} of 10.4nm nanocrystals is on the order of 2×10^{-22} m^2 around the fundamental resonant frequency of (SPH, l=1) modes. It is much less than the measured value of 13nm NCs.

Considering size variation and absorption bandwidth, these peaks match the frequencies of (SPH, l=1, n=0) phonons (Fig. 3(a), solid line) and (SPH, l=1, n=1) phonons (Fig. 3(a), dotted line) and shows inverse dependence on the particle size D (Fig. 3(a)). Removing the contribution from dielectric absorption, the peak σ_{ex} for (SPH, l=1, n=0) modes of 10.4nm, 10.1nm, and 8nm samples are 2×10^{-21} m^2, 1.6×10^{-21} m^2, and 7×10^{-22} m^2, respectively. Together with the σ_{ex} of 13nm NCs, it is worth noting that these data can be fitted by an equation $\sigma_{ex}=aD^4$ (Fig. 3(b), solid curve). According to Murray's electro-mechanical model, the excess THz absorption related to (SPH, l=1) modes can be expressed as $\sigma_{ex}=Q^2/b\varepsilon_0 c$, where b is the friction constant, ε_0 is the permittivity of free space, and c is the speed of light in vacuum.[3] Combining it with our results gives $Q \propto D^2$, indicating the amount of spatial separated charges are proportional to the surface area of NCs. This conclusion is consistent with our proposal that separated charges comes from the surface defect (Tellurium dangling bonds) related donors.

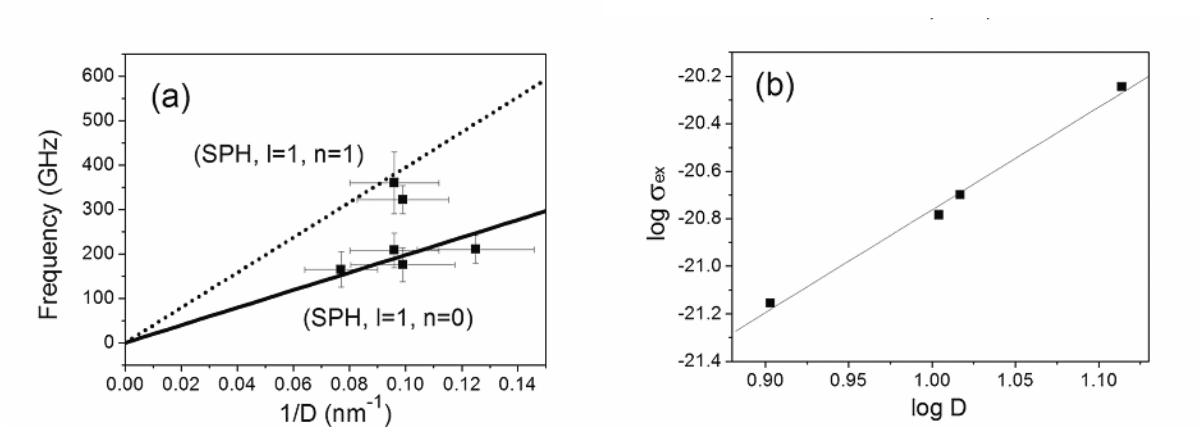

Fig 3. (a) Frequency of (SPH, l=1, n=0) phonons (solid line), (SPH, l=1, n=1) phonons (dotted line), and the THz absorption peaks (solid squares) as a function of inverse nanocrystal size 1/D. The error bars express the size variation and the THz absorption bandwidth. (b) Extinction cross section of excess THz absorption as a function of particle diameter D. The fitting line (solid curve) has a slope of 4.2.

3. USING TYPE-II NANOCRYSTAL AS THE CONTRAST AGENT OF THZ IMAGING

Eexploiting this dipolar resonant absorption feature, type-II nanocrystals can thus serve as the contrast agents for THz imaging. The required absorption contrast at a specific THz frequency can be designed by tailoring the size of the nanocrystals. To demonstrate this idea, we employed a sub-wavelength fiber scanned THz imaging system (See Fig. 4(a)).[11] The imaging frequency was 320GHz, which was determined by the sub-wavelength fiber.[11] As a comparison, we first took the transmission MMW images of three different nanocrystals, which were 4.4nm CdSe, 8nm CdSe/CdTe, and 10.4nm CdSe/CdTe (See Fig. 4(b)). Characterized by their size-dependent dipolar coupling characteristics, only 10.4nm CdSe/CdTe nanocrystals can resonantly absorb 320GHz microwaves, which results in the transmission contrast for the fiber scanned image (dark region of figure 4(c)). We then selected the 10.4nm nanocrystals as a contrast agent and applied them to a bio-sample, a dry sea horse. Before using these contrast agents, the THz transmission image (See Fig. 4(d)) could clearly distinguish the detailed structure inside the body of the dry seahorse including the spine, the brain cavity, the abdominal cavity, and somite. After depositing 10.4nm CdSe/CdTe nanocrystals into the brain cavity, we

could observe obvious contrast from the corresponding MMW image (Fig. 4(e), indicated by a red arrow). This result demonstrates the feasibility that type-II nanocrystals can be used as contrast agents for THz resonant molecular imaging.

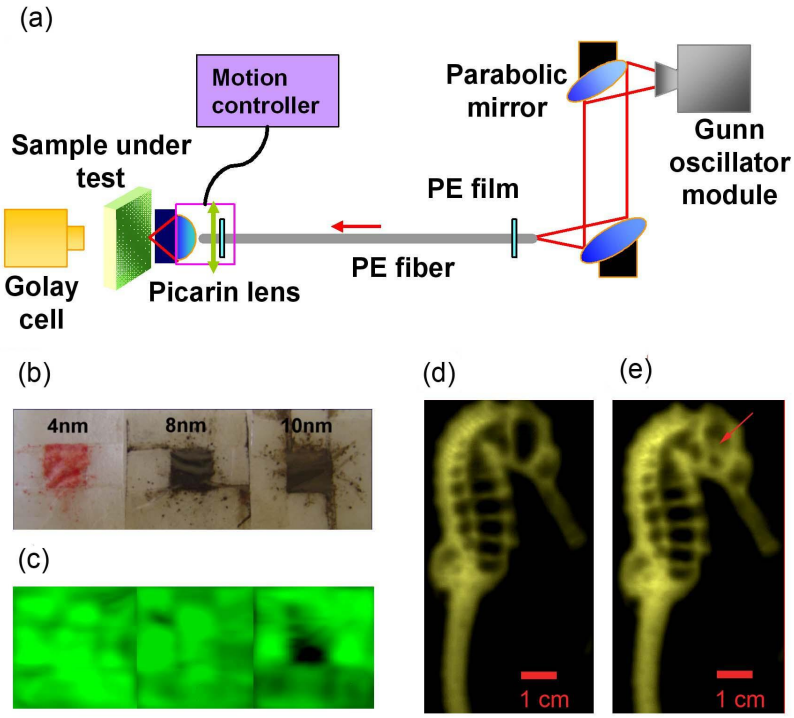

Fig 4. (a) Schematic diagram of subwavelength fiber-scanned THz imaging system. (b) Camera pictures of three different nanocrystals. From left to right, they are powders of 4.4nm CdSe, 8nm CdSe/CdTe, and 10.4nm CdSe/CdTe. (c) THz transmission images of the corresponding nanocrystals listed above. The color green represents high transmission (d) THz transmission images of a bio-sample, a dry sea horse, without contrast agents. The color yellow represents the position where the material has THz absorption. (e) THz transmission images of a dry sea horse with nanocrystals, mimicking contrast agents.

4. THZ PHOTON ABSORPTION BY THE PIEZOELECTRIC NANOCRYSTALS

The above-mentioned symmetry argument assumes that the material is isotropic, this rules out piezoelectric coupling, which might induce THz photon absorption related to the confined acoustic phonons other than [SPH, l=1] modes. To investigate this, we prepared wurtzite (piezoelectric) CdSe nanocrystals for FTIR spectroscopy system to measure their THz photon absorption spectra.

Preparation of the wurtzite CdSe nanocrystals from a CdO green-chemistry precursor was performed according to a method previously reported by Chou and coworkers.[6] The sizes of CdSe nanocrystals could be controlled by terminating the reaction at different times of cooling. The CdSe nanocrystals were then precipitated out from the growth solution by adding methanol. To study the size dependence of THz absorption, we synthesized five batches of CdSe nanocrystals with different sizes. Measuring with a transmission electron microscope, their mean diameters D were found to be 3.4nm, 4.1nm, 4.4nm, 5.6nm, and 5.8nm, respectively, with 10% ~ 20% size variations. To characterize how spherical the particles are, we arbitrarily chose 50 particles from the transmission electron microscope image with nanometer resolution and measured the equatorial and polar radius of the CdSe nanoparticles. The statistical ratio of the short axis over the long axis is 0.91, which is very close to that of a sphere. With a strong confinement of the electronic wave function ($D< 2a_B$~10nm, where a_B is the exciton Bohr radius of CdSe) and a uniform size distribution, we observed clear excitonic absorption (Fig. 5(a)) and sharp ($\delta\lambda$~30nm) photoluminescence peaks (Fig. 5(b)) of the CdSe nanocrystals at room temperature. As the particle size decreased, both the excitonic absorption and the PL peaks blue shifted to shorter

wavelengths (Fig. 5). These results confirm the quality of our samples and are consistent with the trend of size dependency.[12] In order to avoid the THz photon absorption from solutions, we used centrifugation and obtained the powders under nitrogen flow. All of the nanocrystals were wrapped by a passivation layer of TOPO (mass density ρ_m = 880 kg/m^3, longitudinal sound speeds V_{Lm} = 2407 m/s, and transverse sound speeds V_{Tm} = 1203 m/s),[13] which is softer than CdSe (ρ=5810 kg/m^3, longitudinal sound speeds V_L=3570 m/s , and transverse sound speeds V_T=1720m/s).[10] It can be treated as a matrix of the CdSe nanocrystals. The dimensionless actual number of CdSe nanocrystals within the interrogated volume from 3.4nm to 5.8nm nanocrystals were 3.7×10^{17}, 1.6×10^{17}, 7.6×10^{16}, 4.4×10^{16}, and 4.5×10^{16}, respectively. These nanocrystal powders were separately sealed by two poly-ethylene films (30-μm thick) for the convenience of holding in THz photo-absorption measurements. The overall sample thickness was ~500μm.

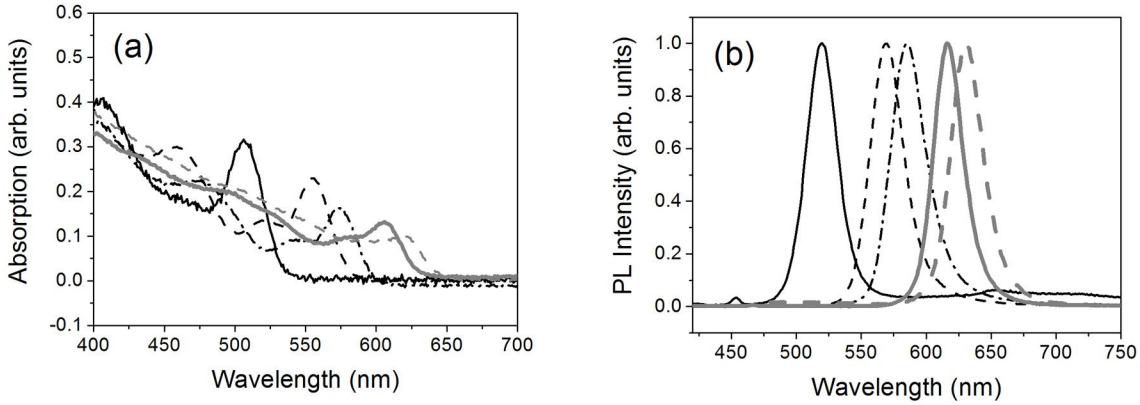

Fig. 5 Room temperature (a) optical absorption and (b) photo-luminescent spectra of CdSe nanocrystals with 3.4nm (solid black), 4.1nm (dashed black), 4.4nm (dash-dotted black), 5.6nm (solid gray), and 5.8nm (dashed gray) particle diameters.

The THz photo-absorption measurements were made by a Bruker IFS 66v Fourier transform infrared spectrometer. For the reduction of water vapor absorption, all the samples were held in a vacuum chamber with 3~4 mbar air pressure. The CdSe samples were illuminated by a THz beam with ~3mm diameter. The transmitted FTIR signals were recorded by a liquid-Helium-cooled silicon bolometer. We first measured the transmitted power spectrum of the poly-ethylene film alone as the background reference. Then we measured the THz photo-absorption spectra of the CdSe nanocrystals with poly-ethylene films at room temperature. The inset of figure 6(a) shows a typical FTIR trace of the 5.8nm sample. Around the frequency of 17.8 cm^{-1} there is an excess absorption dip (indicated by a black arrow) over the background electric-dipole absorption.[5]

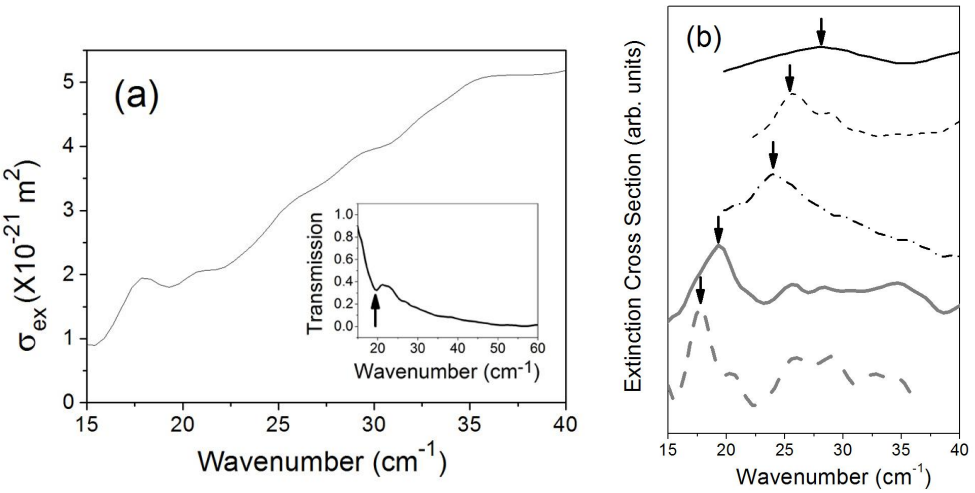

Fig. 6 (a) Extinction-cross-section spectrum of excess THz photon absorption of 5.8nm CdSe nanocrystals, calculated from the transmission spectra (inset figure) measured by a Fourier Transform Infrared (FTIR) spectroscopy system. (b) The

extinction-cross-section spectra of excess THz absorption of CdSe nanocrystals corresponding to the samples characterized in the Figure 5

Then we calculated the corresponding spectrum of the total extinction cross section (See figure 6(a)). By removing the electric-dipole absorption induced background, we can obtain the spectrum of Extinction Cross Section related to the Excess Absorption (ECEA) (Dashed gray trace in Fig. 6(b)). At the maximum of extinction, the ECEA of each 5.8nm CdSe nanocrystal is found to be 6×10^{-22} m^2. With similar measurements and analysis, we also obtained the spectra of ECEA for other sizes of CdSe nanocrystals (Fig. 6(b)). They all show obvious absorption peaks (indicated by arrows) and the frequency of peak absorption blue shifts as the particle size decreases.

To check if the resonant THz absorption originates from the confined acoustic modes, we first calculate the mode frequency ω_o from the eigenfrequency equation for the [SPH, l=0] modes:[1]

$$\tan(\xi_o)(1-\eta_o^{\,2}/4)=\xi_o\,, \tag{2}$$

where $\xi_o=\omega_o D/(2V_L)$ and $\eta_o=\omega_o D/(2V_T)$. Since TOPO is much softer than CdSe, the real part of the eigenfrequency modified by the presence of the TOPO matrix was much smaller than our experimental error. We thus treat the eigenfrequency as ω_o in our following analysis. Another issue is the linewidth broadening. It might result from either homogeneous broadening or inhomogeneous broadening. Homogeneous broadening might come from either finite acsoutic quality factor Q or elastic anisotropy. Using the material parameters of CdSe[10] and TOPO[13], we calculated the acoustic impedance contrast for [SPH, l=0] modes.[14] The resulted Q is around 17.7, To evaluate the contribution from elastic anisotropy, we took the extreme values of the V_L (3505m/s~3793m/s) and the V_T (1506m/s~1840m/s)[15] into Eq.(2). The average variation of eigenfrequency ω_o is about 8%. These results suggest that the broadening of THz absorption linewidth in our measurement should be dominated by the inhomogeneous size distribution, rather than the homogeneous acoustic contrast or elastic anisotropy. Taking the acoustic parameters of CdSe[10] into Eq. (2), we calculate and plot the frequencies of the [SPH, l=0] fundamental mode as a function of the inverse particle diameter in Fig. 7 (solid line). Considering the linewidth broadening effects, good agreement with the experimentally measured THz absorption peak position (open circles) can be found. This result indicates that the excess THz resonant absorption we observed in CdSe nanocrystals are related to the [SPH, l=0] mode, which was originally considered forbidden in non-piezoelectric materials.

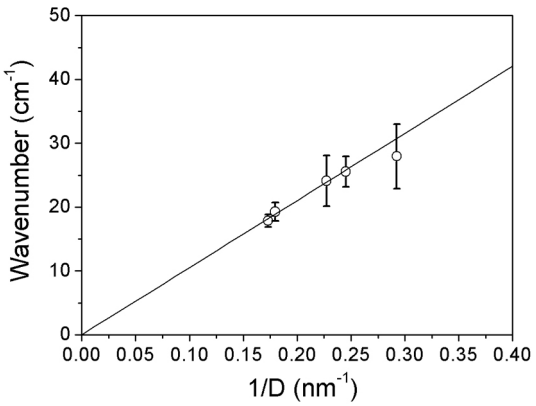

Fig. 7 Frequencies of the measured resonant THz photon absorption peak versus inverse particle diameters of CdSe nanocrystals (open circles). Error bars represent the bandwidth of the resonant absorption. The data points agree well with the calculated eigenfrequency as a function of inverse particle diameter (solid line).

To explore the role that piezoelectric coupling plays in the processes of [SPH, l=0] related THz photon absorption and to estimate the size dependence of this coupling, we developed a theoretical model, where we idealize the CdSe nanocrystals as homogeneous piezoelectric elastic continuum spheres with mass density ρ and radius R. Subjected to an isotropic strain s of [SPH, l=0] breathing mode, the induced polarization is $P_i=e_{ijk}\,s_{jk}$, where e_{ijk} is the piezoelectric constants tensor and s_{jk} is the strain. For the wurtzite (6mm) symmetry, nonzero components of e_{ijk} are e_{31}, e_{33}, and e_{15}.[16] They result in $P_x=P_y=0$ *and* $P_z=(2e_{31}+e_{33})s=\varepsilon_0(\varepsilon_{33}-1)E_z$, where ε_{33} is the relative dielectric constants of CdSe for the

electric field along z-axis. Therefore, the fundamental breathing mode is an excitation which can induce dipole moment change along the z-axis of wurtzite CdSe. The THz photons could thus couple with the breathing mode at its natural resonant frequency ω_o. Since the particle size (3~5nm) is much less than the wavelength of THz electromagnetic waves, we can consider the nanocrystals to be in a quasi-CW electric field. The nanocrystals will thus expand with an increase of radius: $\Delta r = sR = gER$, where g is the coupling factor between the strain and the local electric field E. In addition, the local electric field E in the nanocrystals should be linked to the global electric field E_g with a local field factor f by $E = 3E_g\varepsilon_m/(\varepsilon+2\varepsilon_m) = fE_g$, where ε and ε_m are dielectric constants of CdSe and the matrix, respectively. For time dependent analysis, we followed the treatment used in the Ref. 3. Since the fundamental breathing mode has a radial symmetry, we simplified the formulation by a one dimensional simple harmonic oscillator with force constant k_{sp}. The mass m of the nanocrystals can be linked to k_{sp} by $m\omega_o^2 = k_{sp}$. We also include a damping coefficient b to consider the mechanical coupling of the nanocrystals to the matrix. In the static case, the externally applied force on the simple harmonic oscillator is $F_{ext} = k_{sp}\,\Delta r$. Consequently, $F_{ext} = k_{sp} f E_g\, Rg$, which directly relates the applied electric field E_g to the force driving the simple harmonic oscillator. With this driving force, the equation of motion of the simple harmonic oscillator become:

$$m\frac{d^2r}{dt^2} = F_{ext} - b\frac{dr}{dt} - k_{sp}r\,. \tag{3}$$

Using phasor analysis, we obtain $(k_{sp} + i\omega b - m\omega^2)A = F_{ext}$, where A is the amplitude of r and ω is the frequency of the applied electric field. When $F_{ext} = 0$, the free vibrations are damped and their frequency ω is complex-valued with a positive imaginary part γ, which is equal to $b/(2m)$, and a real part ω_1. The quality factor of the mode Q is $\omega/\Delta\omega$, where γ is equal to $\Delta\omega/2$ and thus Q is equal to $\omega_1/(2\gamma)$. Consequently, the ratio of b over m will be equal to that of ω_1 over Q. At resonance, the time-averaged power absorption by this driven damped simple harmonic oscillator is $P_{avg} = (k_{sp} f E_g Rd_{33})^2/(2b)$.[5] By taking into account the random orientation of the nanoparticles, the effective average value of E^2 is reduced to one third. Accordingly, consider only light damping ($\omega_o \approx \omega_1 = \mathrm{Re}(\eta)V_T/R$), the P_{avg} averaged over the ensemble is $\overline{P_{avg}} = 2\pi\rho Q\,\mathrm{Re}(\eta)^3 V_T^3 f^2 E_g^2 R^2 g^2/9$. Dividing $\overline{P_{avg}}$ by the incident energy flux $S = c\varepsilon_o E_g^2/2$, where c is the speed of light and ε_o is the permittivity in vacuum, the ECEA can be expressed as :

$$\sigma_{ECEA} = \frac{4\pi\rho Q\,\mathrm{Re}(\eta)^3 V_T^3 f^2 R^2 g^2}{9c\varepsilon_o}\,. \tag{4}$$

As described above, soft TOPO won't cause large imaginary part of the eigenfrequency and thus Re(η) is very close to η_0, which is equal to 5.764. The local field factor f is calculated to be 0.54 by the dielectric constant of CdSe (ε=8.82)[17] and TOPO (ε_m=2.5).[18] For a free sphere, the coupling factor g between the strain and the applied electric field can't be larger than that determined by the classical relation of $c_{ijkl}s_{kl} = e_{ijk}E_k$, where c_{ijkl} is the stiffness constants. The corresponding g is equal to the element of e_{ijk} devided by c_{ijkl}, which is on the order of 4×10^{-12} C/N for CdSe.[15] Inserting all these numerical factors and material parameters of CdSe into Eq. (4), σ_{ECEA} are found to be around 10^{-21} m^2, which are on the same order with our measured results (Fig. 4, solid squares). From the log 10-log 10 plot of σ_{ECEA} (Fig. 8) versus the particle diameters, the data fitting line has a slope of 2.3, which is close to our theoretically prediction that σ_{ECEA} is proportional to R^2. These results support our hypothesis that the piezoelectric coupling would induce excess THz resonant absorption with the breathing modes of the CdSe nanocrystals.

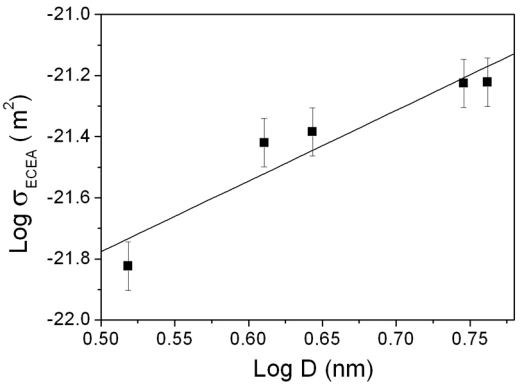

Fig. 8 Log 10- log 10 plot of the measured extinction cross-section of excess THz photon absorbtion vs the particle diameters of CdSe nanocrystals (solid squares). The fitting line (solid curve) is with a slope of 2.3.

5. SUMMARY

In conclusion, with specific charge separation in CdSe/CdTe type-II nanocrystals, we successfully induced THz resonant photon absorption related to [SPH, l=1] confined acoustic modes. Exploiting this characteristic absorption, by tailoring the size of nanocrystals, type-II nanocrystals can serve as contrast agents for THz imaging. With CdSe nanocrystals we also observed the first piezoelectric coupled THz resonant photon absorption related to the confined acoustic modes in nanoparticles. By measuring the FTIR spectra of the CdSe nanocrystals with different sizes, we showed that the frequencies are in agreement with the [SPH, l=0] breathing modes predicted by the elastic continuum theory. Our result suggests new mechanisms for low dimensional systems to convert a THz photon into a phonon of the same frequency.

6. ACKNOWLEDGEMENTS

This project is sponsored by the National Science Council of Taiwan under grant numbers of **NSC96-2120-M-002-014** and **NSC 96-2628-E-002-043-MY3** and by the National Taiwan University Research Center for Medical Excellence. We thank D. B. Murray and L. Saviot for technical discussions on the dipolar modes in a nanosphere.

REFERENCES

[1] Lamb, H., "On the vibrations of an elastic sphere," Proc. London Math. Soc. **13**, 189-212 (1882).
[2] Duval, E., "Far-infrared and Raman vibrational transitions of a solid sphere: Selection rules," Phys. Rev. B **46**(9), 5795-5797 (1992).
[3] Murray, D. B., Netting, C. H., Saviot, L., Pighini, C., Millot, N., Aymes, D., and Liu, H.-L., "Far-infrared absorption by acoustic phonons in Titanium dioxide nanopowders," J. Nanoelectron. Optoelectron. **1**(1), 92-98 (2006).
[4] Kim, S., Fisher, B., Eisler, H.-J., and Bawendi, M., "Type-II quantum dots: CdTe/CdSe (core/shell) and CdSe/ZnTe (core/shell) heterostructures," J. Am. Chem. Soc. **125**(38), 11466-11467 (2003).
[5] Lee, S.-I., Noh, T. W., Cummings, K., and Gaines, J. R., "Far-infrared absorption of silver-particle composites," Phys. Rev. Lett. **55**(15), 1626-1629 (1985).
[6] Chen, C.-Y., Cheng, C.-T., Lai, C.-W., Hu, Y.-H., Chou, P.-T., Chou, Y.-H., and Chiu, H.-T., "Tepe-II CdSe/CdTe/ZnTe(core-shell-shell) quantum dots with cascade band edges: the separation of electron (at CdSe) and hole (ZnTe) by the CdTe layer," Small **1**(12), 1215-1220 (2005).
[7] Poznyak, S. K., Osipovich, N. P., Shavel, A., Talapin, D. V., Gao, M., Eychmüller, A., and Gaponik, N., "Size-dependent electrochemical behavior of thiol-capped CdTe nanocrystals in aqueous solution," J. Phys. Chem. B **109**(3), 1094-1100 (2005).
[8] Lu, J.-Y., Chen, L.-J., Kao, T.-F., Chang, H.-H., Chen, H.-W., Liu, A.-S., Chen,Y.-C., Wu, R.-B., Liu, W.-S., Chyi, J.-I., and Sun, C.-K., "Terahertz microchip for illicit drug detection," IEEE Photon. Technol. Lett. **18**(21-24), 2254-2256 (2006).
[9] Pan, C.-L., Hsieh, C.-F., Pan, R.-P., Tanaka, M., Miyamaru, F., Tani, M., and Hangyo, M., "Control of enhanced THz transmission through metallic hole arrays using nematic liquid crystal," Opt. Express **13**(11), 3921-3930 (2005).
[10] Rode, D. L., "Electron mobility in II-VI semiconductors," Phys. Rev. B **2**(10), 4036 (1970).
[11] Chen L.-J., Chen H.-W., Kao T.-F., Lu J.-Y., Sun C.-K., "Low-loss subwavelength plastic fiber for terahertz waveguiding, " *Opt. Lett.* **31**(3), 308-310 (2006).
[12] Murphy, C. J., "Optical sensing with quantum dots," *Anal.Chem.* **74**(19), 520A-526A (2002).

[13] Banerjee, S., Jia, S., Kim, D. I., Robinson, R. D., Kysar, J. W., Bevk, J., and Herman, I. P., "Raman microprobe analysis of elastic strain and fracture in electrophoretically deposited CdSe nanocrystal films," *Nano Lett.* **6**(2), 175-180 (2006).
[14] Saviot, L. and Murray, D. B., "Long lived acoustic vibrational modes of an embedded nanoparticles," *Phys. Rev. Lett.* **93**(5), 055506 (2004).
[15] Zubritskiĭ, V. V., "Phonon focusing in CdSe, ZnS, and ZnO crystals," Tech. Phys. **42**(6), 639-643 (1997).
[16] Royer, D. and Dieulesaint, E., [Elastic Waves in Solids I], Springer-Verlag, Berlin Heidelberg, Ch. 3 (2000).
[17] Beard, M. C., Turner, G. M., and Schmuttenmaer, C. A., "Size-dependent photoconductivity in CdSe nanoparticles as measured by time-resolved terahertz spectroscopy," *Nano Lett.* **2**(9), 983-987 (2002).
[18] Jiang, J., Krauss, T. D., and Brus, L. E., "Electrostatic force microscopy characterization of trioctylphosphine oxide self-assembled monolayers on graphite," *J. Phys. Chem. B* **104**(50), 11936-11941 (2000).